4

Study of LCC Resonant Transistor DC / DC Converter with Capacitive Output Filter

Nikolay Bankov, Aleksandar Vuchev and Georgi Terziyski
University of Food Technologies – Plovdiv
Bulgaria

1. Introduction

The transistor LCC resonant DC/DC converters of electrical energy, working at frequencies higher than the resonant one, have found application in building powerful energy supplying equipment for various electrical technologies (Cheron et al., 1985; Malesani et al., 1995; Jyothi & Jaison, 2009). To a great extent, this is due to their remarkable power and mass-dimension parameters, as well as, to their high operating reliability. Besides, in a very wide-working field, the LCC resonant converters behave like current sources with big internal impedance. These converters are entirely fit for work in the whole range from no-load to short circuit while retaining the conditions for soft commutation of the controllable switches.

There is a multitude of publications, dedicated to the theoretical investigation of the LCC resonant converters working at a frequency higher than their resonant one (Malesani et al., 1995; Ivensky et al. 1999). In their studies most often the first harmonic analysis is used, which is practically precise enough only in the field of high loads of the converter. With the decrease in the load the mistakes related to using the method of the first harmonic could obtain fairly considerable values.

During the analysis, the influence of the auxiliary (snubber) capacitors on the controllable switches is usually neglected, and in case of availability of a matching transformer, only its transformation ratio is taken into account. Thus, a very precise description of the converter operation in a wide range of load changes is achieved. However, when the load resistance has a considerable value, the models created following the method mentioned above are not correct. They cannot be used to explain what the permissible limitations of load change depend on in case of retaining the conditions for soft commutation at zero voltage of the controllable switches – zero voltage switching (ZVS).

The aim of the present work is the study of a transistor LCC resonant DC/DC converter of electrical energy, working at frequencies higher than the resonant one. The possible operation modes of the converter with accounting the influence of the damping capacitors and the parameters of the matching transformer are of interest as well. Building the output characteristics based on the results from a state plane analysis and suggesting a methodology for designing, the converter is to be done. Drawing the boundary curves between the different operating modes of the converter in the plane of the output characteristics, as well as outlining the area of natural commutation of the controllable switches are also among the aims of this work. Last but not least, the work aims at designing and experimental investigating a laboratory prototype of the LCC resonant converter under consideration.

2. Modes of operation of the converter

The circuit diagram of the LCC transistor resonant DC/DC converter under investigation is shown in figure 1. It consists of an inverter (controllable switches constructed on base of the transistors $Q_1 \div Q_4$ with freewheeling diodes $D_1 \div D_4$), a resonant circuit (L, C), a matching transformer Tr, an uncontrollable rectifier ($D_5 \div D_8$), capacitive input and output filters (C_{F1} и C_{F2}) and a load resistor (R_0). The snubber capacitors ($C_1 \div C_4$) are connected with the transistors in parallel.

The output power of the converter is controlled by changing the operating frequency, which is higher than the resonant frequency of the resonant circuit.

It is assumed that all the elements in the converter circuit (except for the matching transformer) are ideal, and the pulsations of the input and output voltages can be neglected.

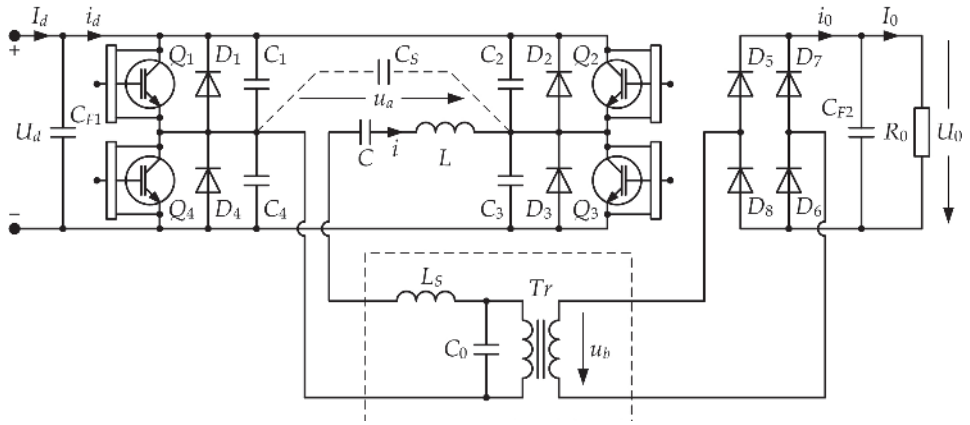

Fig. 1. Circuit diagram of the LCC transistor DC/DC converter

All snubber capacitors $C_1 \div C_4$ are equivalent in practice to just a single capacitor C_S (dotted line in fig.1), connected in parallel to the output of the inverter. The capacity of the capacitor C_S is equal to the capacity of each of the snubber capacitors $C_1 \div C_4$.

The matching transformer Tr is shown in fig.1 together with its simplified equivalent circuit under the condition that the magnetizing current of the transformer is negligible with respect to the current in the resonant circuit. Then this transformer comprises both the full leakage inductance L_S and the natural capacity of the windings C_0, reduced to the primary winding, as well as an ideal transformer with its transformation ratio equal to k.

The leakage inductance L_S is connected in series with the inductance of the resonant circuit L and can be regarded as part of it. The natural capacity C_0 takes into account the capacity between the windings and the different layers in each winding of the matching transformer. C_0 can has an essential value, especially with stepping up transformers (Liu et al., 2009).

Together with the capacity C_0 the resonant circuit becomes a circuit of the third order (L, C and C_0), while the converter could be regarded as LCC resonant DC/DC converter with a capacitive output filter.

The parasitic parameters of the matching transformer – leakage inductance and natural capacity of the windings – should be taken into account only at high voltages and high operating frequencies of the converter. At voltages lower than 1000 V and frequencies lower

than 100 kHz they can be neglected, and the capacitor C_0 should be placed additionally (Liu et al., 2009).

Because of the availability of the capacitor C_S , the commutations in the output voltage of the inverter (u_a) are not instantaneous. They start with switching off the transistors Q_1/Q_3 or Q_2/Q_4 and end up when the equivalent snubber capacitor is recharged from $+U_d$ to $-U_d$ or backwards and the freewheeling diodes D_2/D_4 or D_1/D_3 start conducting. In practice the capacitors C_2 and C_4 discharge from $+U_d$ to 0, while C_1 and C_3 recharge from 0 to$+U_d$ or backwards. During these commutations, any of the transistors and freewheeling diodes of the inverter does not conduct and the current flowed through the resonant circuit is closed through the capacitor C_S.

Because of the availability of the capacitor C_0, the commutations in the input voltage of the rectifier (u_b) are not instantaneous either. They start when the diode pairs (D_5/D_7 or D_6/D_8) stop conducting at the moments of setting the current to zero through the resonant circuit and end up with the other diode pair (D_6/D_8 *или* D_5/D_7) start conducting, when the capacitor C_0 recharges from $+kU_0$ to $-kU_0$ or backwards. During these commutations, any of the diodes of the rectifier does not conduct and the current flowed through the resonant circuit is closed through the capacitor C_0.

The condition for natural switching on of the controllable switches at zero voltage (ZVS) is fulfilled if the equivalent snubber capacitor C_S always manages to recharge from $+U_d$ to $-U_d$ or backwards. At modes, close to no-load, the recharging of C_S is possible due to the availability of the capacitor C_0. It ensures the flow of current through the resonant circuit, even when the diodes of the rectifier do not conduct.

When the load and the operating frequency are deeply changed, three different operation modes of the converter can be observed.

It is characteristic for the first mode that the commutations in the rectifier occur entirely in the intervals for conducting of the transistors in the inverter. This mode *is the main operation mode* of the converter. It is observed at comparatively small values of the load resistor R_0.

At the second mode the commutation in the rectifier ends during the commutation in the inverter, i.e., the rectifier diodes start conducting when both the transistors and the freewheeling diodes of the inverter are closed. This is *the medial operation mode* and it is only observed in a narrow zone, defined by the change of the load resistor value which is however not immediate to no-load.

At modes, which are very close to no-load the third case is observed. The commutations in the rectifier now complete after the ones in the inverter, i.e. the rectifier diodes start conducting after the conduction beginning of the corresponding inverter's freewheeling diodes. This mode is *the boundary operation mode* with respect to no-load.

3. Analysis of the converter

In order to obtain general results, it is necessary to normalize all quantities characterizing the converter's state. The following quantities are included into relative units:

$x = U'_C = u_C/U_d$ - Voltage of the capacitor *C*;

$y = I' = \dfrac{i}{U_d/Z_0}$ - Current in the resonant circuit;

$U'_0 = kU_0/U_d$ - Output voltage;

$I_0' = \dfrac{I_0/k}{U_d/Z_0}$ - Output current;

$U_{Cm}' = U_{Cm}/U_d$ - Maximum voltage of the capacitor *C*;

$\nu = \omega/\omega_0$ - Distraction of the resonant circuit,

where ω is the operating frequency and $\omega_0 = 1/\sqrt{LC}$ and $Z_0 = \sqrt{L/C}$ are the resonant frequency and the characteristic impedance of the resonant circuit *L*-*C* correspondingly.

3.1 Analysis at the main operation mode of the converter

Considering the influence of the capacitors C_S and C_0, the main operation mode of the converter can be divided into eight consecutive intervals, whose equivalent circuits are shown in fig. 2. By the trajectory of the depicting point in the state plane $(x = U_C'; y = I')$, shown in fig. 3, the converter's work is also illustrated, as well as by the waveform diagrams in fig.4.

The following four centers of circle arcs, constituting the trajectory of the depicting point, correspond to the respective intervals of conduction by the transistors and freewheeling diodes in the inverter: interval 1: Q_1/Q_3 - $(1-U_0';0)$; interval 3: D_2/D_4 - $(-1-U_0';0)$; interval 5: Q_2/Q_4 - $(-1+U_0';0)$; interval 7: D_1/D_3 - $(1+U_0';0)$.

The intervals 2 and 6 correspond to the commutations in the inverter. The capacitors *C* and C_S then are connected in series and the sinusoidal quantities have angular frequency of $\omega_0' = 1/\sqrt{LC_{E1}}$ where $C_{E1} = CC_S/(C+C_S)$. For the time intervals 2 and 6 the input current i_d is equal to zero. These pauses in the form of the input current i_d (fig. 4) are the cause for increasing the maximum current value through the transistors but they do not influence the form of the output characteristics of the converter.

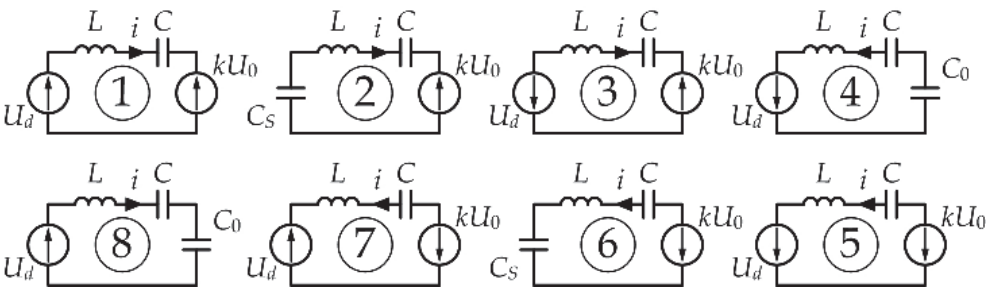

Fig. 2. Equivalent circuits at the main operation mode of the converter.

The intervals 4 and 8 correspond to the commutations in the rectifier. The capacitors *C* and C_0 are then connected in series and the sinusoidal quantities have angular frequency of $\omega_0'' = 1/\sqrt{LC_{E2}}$ where $C_{E2} = CC_0/(C+C_0)$. For the time intervals 4 and 8, the output current i_0 is equal to zero. Pauses occur in the form of the output current i_0, decreasing its average value by ΔI_0 (fig. 4) and essentially influence the form of the output characteristics of the converter.

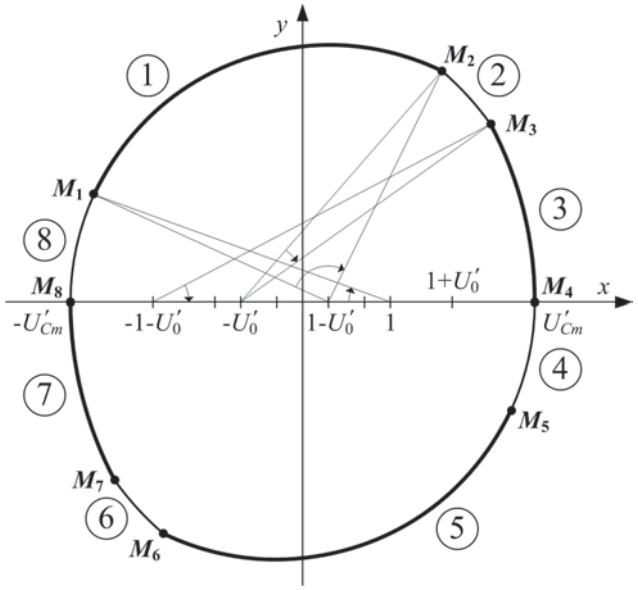

Fig. 3. Trajectory of the depicting point at the main mode of the converter operation.

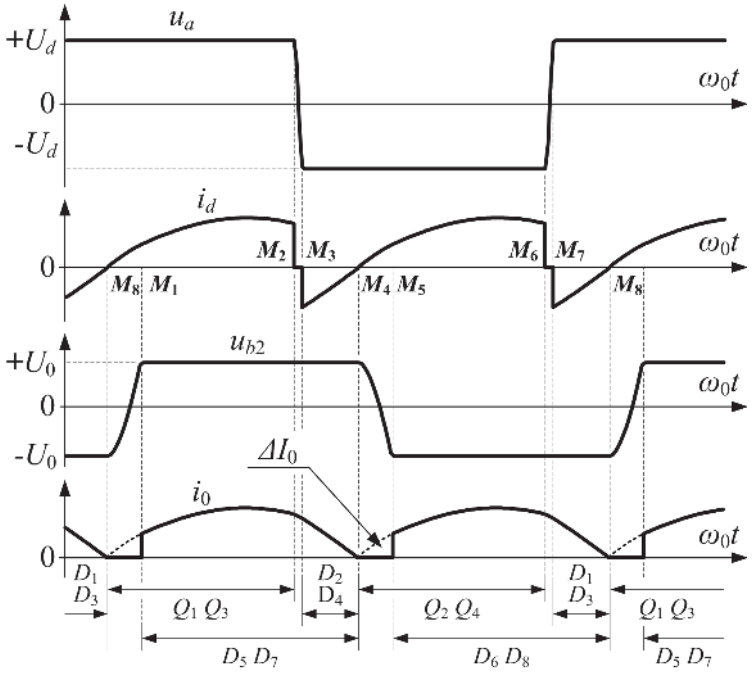

Fig. 4. Waveforms of the voltages and currents at the main operation mode of the converter

It has been proved in (Cheron, 1989; Bankov, 2009) that in the state plane (fig. 3) the points, corresponding to the beginning (p.M_2) and the end (p.M_3) of the commutation in the inverter belong to the same arc with its centre in point $(-U_0';0)$. It can be proved the same way that the points, corresponding to the beginning (p.M_8) and the end (p.M_1) of the commutation in the rectifier belong to an arc with its centre in point $(1;0)$. It is important to note that only the end points are of importance on these arcs. The central angles of these arcs do not matter either, because as during the commutations in the inverter and rectifier the electric quantities change correspondingly with angular frequencies ω_0' and ω_0'', not with ω_0.
The following designations are made:

$$a_1 = C_S/C \qquad n_1 = \sqrt{(a_1+1)/a_1} \tag{1}$$

$$a_2 = C_0/C \qquad n_2 = \sqrt{(a_2+1)/a_2} \tag{2}$$

$$n_3 = \sqrt{1+1/a_1+1/a_2} \tag{3}$$

For the state plane shown in fig, 3 the following dependencies are valid:

$$(x_1 - 1 + U_0')^2 + y_1^2 = (x_2 - 1 + U_0')^2 + y_2^2 \tag{4}$$

$$(x_2 + U_0')^2 + y_2^2 = (x_3 + U_0')^2 + y_3^2 \tag{5}$$

$$(x_3 + 1 + U_0')^2 + y_3^2 = (x_4 + 1 + U_0')^2 + y_4^2 \tag{6}$$

$$(x_4 + 1)^2 + y_4^2 = (x_5 + 1)^2 + y_5^2 \tag{7}$$

From the existing symmetry with respect to the origin of the coordinate system of the state plane it follows:

$$x_5 = -x_1 \tag{8}$$

$$y_5 = -y_1 \tag{9}$$

During the commutations in the inverter and rectifier, the voltages of the capacitors C_S and C_0 change correspondingly by the values $2U_d$ and $2kU_0$, and the voltage of the commutating capacitor C changes respectively by the values $2a_1U_d$ and $2a_2kU_0$. Consequently:

$$x_3 = x_2 + 2a_1 \tag{10}$$

$$x_5 = x_4 - 2a_2U_0' \tag{11}$$

The equations (4)÷(11) allow for calculating the coordinates of the points M_1÷M_4 in the state plane, which are the starting values of the current through the inductor L and the voltage of

the commutating capacitor C in relative units for each interval of converter operation. The expressions for the coordinates are in function of U'_0, U'_{Cm}, a_1 and a_2:

$$x_1 = -U'_{Cm} + 2a_2U'_0 \tag{12}$$

$$y_1 = \sqrt{4a_2U'_0\left(U'_{Cm} - a_2U'_0 + 1\right)} \tag{13}$$

$$x_2 = U'_0U'_{Cm} - a_2U'^2_0 - a_1 \tag{14}$$

$$y_2 = \sqrt{\begin{matrix}\left(-U'_{Cm} + 2a_2U'_0 - U'_0U'_{Cm} + a_2U'^2_0 + a_1\right)\cdot \\ \cdot\left(-U'_{Cm} + 2a_2U'_0 + U'_0U'_{Cm} - a_2U'^2_0 - a_1 + 2U'_0 - 2\right) + \\ +4a_2U'_0\left(U'_{Cm} - a_2U'_0 + 1\right)\end{matrix}} \tag{15}$$

$$x_3 = U'_0U'_{Cm} - a_2U'^2_0 + a_1 \tag{16}$$

$$y_3 = \sqrt{\begin{matrix}\left(U'_{Cm} - U'_0U'_{Cm} + a_2U'^2_0 - a_1\right)\cdot \\ \cdot\left(U'_{Cm} + U'_0U'_{Cm} - a_2U'^2_0 + a_1 + 2U'_0 + 2\right)\end{matrix}} \tag{17}$$

$$x_4 = U'_{Cm} \tag{18}$$

$$y_4 = 0 \tag{19}$$

For converters with only two reactive elements (L and C) in the resonant circuit the expression for its output current I'_0 is known from (Al Haddad et al., 1986; Cheron, 1989):

$$I'_0 = 2\nu U'_{C1m}/\pi \tag{20}$$

The LCC converter under consideration has three reactive elements in its resonant circuit (L, C и C_0). From fig.4 it can be seen that its output current I'_0 decreases by the value $\Delta I'_0 = 2a_2\nu U'_0/\pi$:

$$I'_0 = 2\nu U'_{Cm}/\pi - \Delta I'_0 = 2\nu\left(U'_{Cm} - a_2U'_0\right)/\pi \tag{21}$$

The following equation is known:

$$\frac{\pi}{\nu} = \omega_0\left(t_1 + t_2 + t_3 + t_4\right), \tag{22}$$

where the times t_1÷t_4 represent the durations of the different stages – from 1 to 4.
For the times of the four intervals at the main mode of operation of the converter within a half-cycle the following equations hold:

$$t_1 = \frac{1}{\omega_0}\left(arctg\frac{y_2}{-x_2 + 1 - U'_0} - arctg\frac{y_1}{-x_1 + 1 - U'_0}\right) \tag{23a}$$

at $x_2 \le 1 - U_0'$ and $x_1 \le 1 - U_0'$

$$t_1 = \frac{1}{\omega_0}\left(\pi - arctg\frac{y_2}{x_2 - 1 + U_0'} - arctg\frac{y_1}{-x_1 + 1 - U_0'}\right) \tag{23b}$$

at $x_2 \ge 1 - U_0'$ and $x_1 \le 1 - U_0'$

$$t_1 = \frac{1}{\omega_0}\left(arctg\frac{y_2}{-x_2 + 1 - U_0'} + arctg\frac{y_1}{x_1 - 1 + U_0'}\right) \tag{23c}$$

at $x_2 \ge 1 - U_0'$ and $x_1 \ge 1 - U_0'$

$$t_2 = \frac{1}{n_1\omega_0}\left(arctg\frac{n_1 y_2}{x_2 - 1 + U_0'} - arctg\frac{n_1 y_3}{x_3 + 1 + U_0'}\right) \tag{24a}$$

at $x_2 \ge 1 - U_0'$

$$t_2 = \frac{1}{n_1\omega_0}\left(arctg\frac{n_1 y_2}{x_2 - 1 + U_0'} - arctg\frac{n_1 y_3}{x_3 + 1 + U_0'}\right) \tag{24b}$$

at $x_2 \le 1 - U_0'$

$$t_3 = \frac{1}{\omega_0} arctg\frac{y_3}{x_3 + 1 + U_0'} \tag{25}$$

$$t_4 = \frac{1}{n_2\omega_0}\left(arctg\frac{n_2 y_1}{-x_1 + 1 - U_0'}\right) \tag{26a}$$

at $x_1 \le 1 - U_0'$

$$t_4 = \frac{1}{n_2\omega_0}\left(\pi - arctg\frac{n_2 y_1}{x_1 - 1 + U_0'}\right) \tag{26b}$$

at $x_1 \ge 1 - U_0'$

It should be taken into consideration that for stages 1 and 3 the electric quantities change with angular frequency ω_0, while for stages 2 and 4 – the angular frequencies are respectively $\omega_0' = n_1\omega_0$ and $\omega_0'' = n_2\omega_0$.

3.2 Analysis at the boundary operation mode of the converter

At this mode, the operation of the converter for a cycle can be divided into eight consecutive stages (intervals), whose equivalent circuits are shown in fig. 5. It makes impression that the sinusoidal quantities in the different equivalent circuits have three different angular frequencies:

$\omega_0 = 1/\sqrt{LC}$ for stages 4 and 8;
$\omega_0'' = 1/\sqrt{LC_{E2}}$, where $C_{E2} = CC_0/(C+C_0)$, for stages 1, 3, 5 and 7;
$\omega_0''' = 1/\sqrt{LC_{E3}}$, where $C_{E3} = CC_SC_0/(CC_S + CC_0 + C_SC_0)$, for stages 2 and 6.

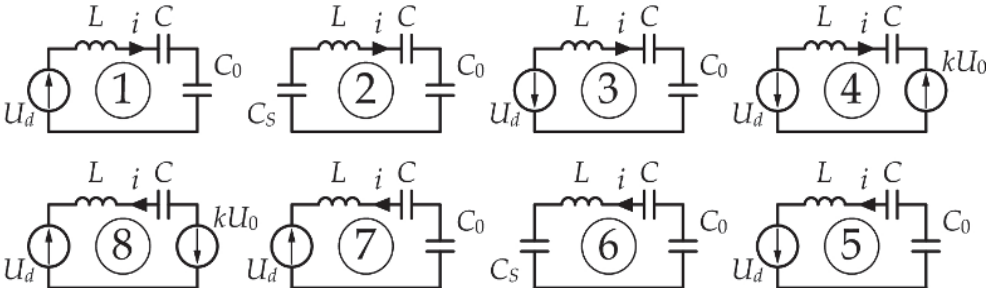

Fig. 5. Equivalent circuits at the boundary operation mode of the converter

In this case the representation in the state plane becomes complex and requires the use of two state planes (fig.6). One of them is $(x = U_C'; y = I')$ and it is used for presenting stages 4 and 8, the other is $(x^0; y^0)$, where:

$$x^0 = u_{C_{E2}}/U_d\,; \qquad y^0 = \frac{i}{U_d/\sqrt{L/C_{E2}}}\,.$$

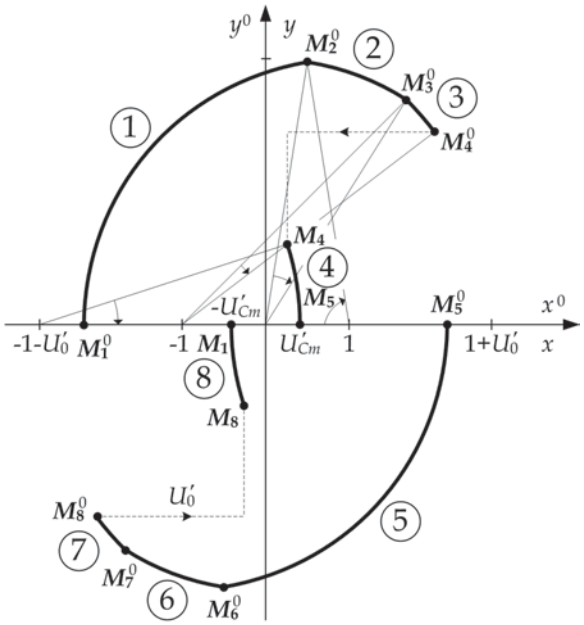

Fig. 6. Trajectory of the depicting point at the boundary mode of operation of the converter

Stages 2 and 6 correspond to the commutations in the inverter.
The commutations in the rectifier begin in p. M_1^0 or p. M_5^0 and end in p. M_4^0 or p. M_8^0, comprising stages 1,2 and 3 or 5,6 and 7.
The transistors conduct for the time of stages 1 and 5, the freewheeling diodes – for the time of stages 3, 4, 7 and 8, and the rectifier diodes – for the time of stages 4 and 8.
The following equations are obtained in correspondence with the trajectory of the depicting point for this mode of operation (fig.6):

$$\left(1-x_1^0\right)^2=\left(1-x_2^0\right)^2+\left(y_2^0\right)^2 \tag{27}$$

$$\left(x_2^0\right)^2+\left(y_2^0\right)^2=\left(x_3^0\right)^2+\left(y_3^0\right)^2 \tag{28}$$

$$\left(x_3^0+1\right)^2+\left(y_3^0\right)^2=\left(x_4^0+1\right)^2+\left(y_4^0\right)^2 \tag{29}$$

$$\left(x_4+1+U_0'\right)^2+\left(y_4\right)^2=\left(1+U_0'-x_1\right)^2 \tag{30}$$

During the commutations in the inverter, the voltage of the capacitor C_{E2} changes by the value $2U_dC_S/C_{E2}$ and consequently:

$$x_3^0=x_2^0+2a_1n_2^2 \tag{31}$$

The same way during the commutation in the rectifier, the voltage of the capacitor C_{E2} changes by the value $2kU_0C_0/C_{E2}$ and consequently:

$$x_4^0=x_1^0+2U_0'\left(1+a_2\right) \tag{32}$$

From the principle of continuity of the current through the inductor L and of the voltage in the capacitor C it follows:

$$x_4^0=x_4+U_0' \tag{33}$$

$$y_4^0=n_2y_4 \tag{34}$$

where $\left(x_i;y_i\right)$ and $\left(x^0{}_i;y^0{}_i\right)$ are the coordinates of M_i and M_i^0 respectively.
The equations (27)÷(34) allow for defining the coordinates of the points $M_1^0 \div M_4^0$ in the state plane:

$$x_1^0=-U_{Cm}'-U_0' \tag{35}$$

$$y_1^0=0 \tag{36}$$

$$x_2^0=\frac{\left(U_{Cm}'-a_2U_0'\right)\left(1+U_0'+a_2U_0'\right)}{a_2}-a_1n_2^2 \tag{37}$$

$$y_2^0 = \sqrt{\left(U'_{Cm} + 1 + U'_o\right)^2 - \left(1 - x_2^0\right)^2} \tag{38}$$

$$x_3^0 = \frac{\left(U'_{Cm} - a_2 U'_0\right)\left(1 + U'_0 + a_2 U'_0\right)}{a_2} + a_1 n_2^2 \tag{39}$$

$$y_3^0 = \sqrt{\left(x_2^0\right)^2 + \left(y_2^0\right)^2 - \left(x_3^0\right)^2} \tag{40}$$

$$x_4^0 = -U'_{Cm} + U'_0\left(1 + 2a_2\right) \tag{41}$$

$$y_4^0 = 2\sqrt{\left(a_2 U'_0 + 1 + U'_0\right)\left(a_2 U'_0 - U'_{Cm}\right)} \tag{42}$$

At the boundary operation mode the output current I'_0 is defined by expression (21) again, where $t_1 \div t_4$ represent the times of the different stages – from 1 to 4.
For the times of the four intervals at the boundary operation mode of the converter within a half-cycle the following equations hold:

$$t_1 = \frac{1}{n_2\omega_0}\left(arctg\frac{y_2^0}{1 - x_2^0}\right) \qquad \text{at } x_2^0 \le 1 \tag{43a}$$

$$t_1 = \frac{1}{n_2\omega_0}\left(\pi - arctg\frac{y_2^0}{x_2^0 - 1}\right) \qquad \text{at } x_2^0 \ge 1 \tag{43b}$$

$$t_2 = \frac{1}{n_3\omega_0}\left(\pi - arctg\frac{n_3 y_2^0}{n_2\left(1 - x_2^0\right)} - arctg\frac{n_3 y_3^0}{n_2\left(1 + x_3^0\right)}\right) \qquad \text{at } x_2^0 \le 1 \tag{44a}$$

$$t_2 = \frac{1}{n_3\omega_0}\left(arctg\frac{n_3 y_2^0}{n_2\left(x_2^0 - 1\right)} - arctg\frac{n_3 y_3^0}{n_2\left(1 + x_3^0\right)}\right) \qquad \text{at } x_2^0 \ge 1 \tag{44b}$$

$$t_3 = \frac{1}{n_2\omega_0}\left(arctg\frac{y_3^0}{1 + x_3^0} - arctg\frac{y_4^0}{1 + x_4^0}\right) \tag{45}$$

$$t_4 = \frac{1}{\omega_0}\left(arctg\frac{y_4}{x_4 + 1 + U'_0}\right) \tag{46}$$

It should be taken into consideration that for stages 1 and 3 the electric quantities change by angular frequency $\omega''_0 = n_2\omega_0$, while for stages 2 and 4 the angular frequencies are correspondingly $\omega'''_0 = n_3\omega_0$ and ω_0.

4. Output characteristics and boundary curves

On the basis of the analysis results, equations for the output characteristics are obtained individually for both the main and the boundary modes of the converter operation. Besides, expressions for the boundary curves of the separate modes are also derived.

4.1 Output characteristics and boundary curves at the main operation mode

From equation (21) U'_{Cm} is expressed in function of U'_0, I'_0, ν and a_2

$$U'_{Cm} = \frac{\pi}{2\nu} I'_0 + a_2 U'_0 \tag{47}$$

By means of expression (47) U'_{Cm} is eliminated from the equations (12)÷(18). After consecutive substitution of expressions (12)÷(18) in equations (23)÷(26) as well as of expressions (23)÷(26) in equation (22), an expression of the kind $U'_0 = f(I'_0, \nu, a_1, a_2)$ is obtained. Its solution provides with the possibility to build the output characteristics of the converter in relative units at the main mode of operation and at regulation by means of changing the operating frequency. The output characteristics of the converter respectively for ν=1.2; 1.3; 1.4; 1.5; 1.8; 2.5; 3.0; 3.3165; 3,6 and a_1=0.1; a_2=0.2 as well as for ν=1.2; 1.3; 1.4; 1.5; 1.6; 1.8 and a_1=0.1; a_2=1.0 are shown in fig.7-a and 7-b.

The comparison of these characteristics to the known ones from (Al Haddad et al., 1986; Cheron, 1989) shows the entire influence of the capacitors C_S и C_0. It can be seen that the output characteristics become more vertical and the converter can be regarded to a great extent as a source of current, stable at operation even at short circuit. Besides, an area of operation is noticeable, in which $U'_0 > 1$.

At the main operation mode the commutations in the rectifier (stages 4 and 8) must always end before the commutations in the inverter have started. This is guaranteed if the following condition is fulfilled:

$$x_1 \le x_2 \tag{48}$$

In order to enable natural switching of the controllable switches at zero voltage (ZVS), the commutations in the inverter (stages 2 and 6) should always end before the current in the resonant circuit becomes zero. This is guaranteed if the following condition is fulfilled:

$$x_3 \le U'_{Cm} \tag{49}$$

If the condition (49) is not fulfilled, then switching a pair of controllable switches off does not lead to natural switching the other pair of controllable switches on at zero voltage and then the converter stops working. It should be emphasized that these commutation mistakes do not lead to emergency modes and they are not dangerous to the converter. When it „misses", all the semiconductor switches stop conducting and the converter just stops working. This is one of the big advantages of the resonant converters working at frequencies higher than the resonant one.

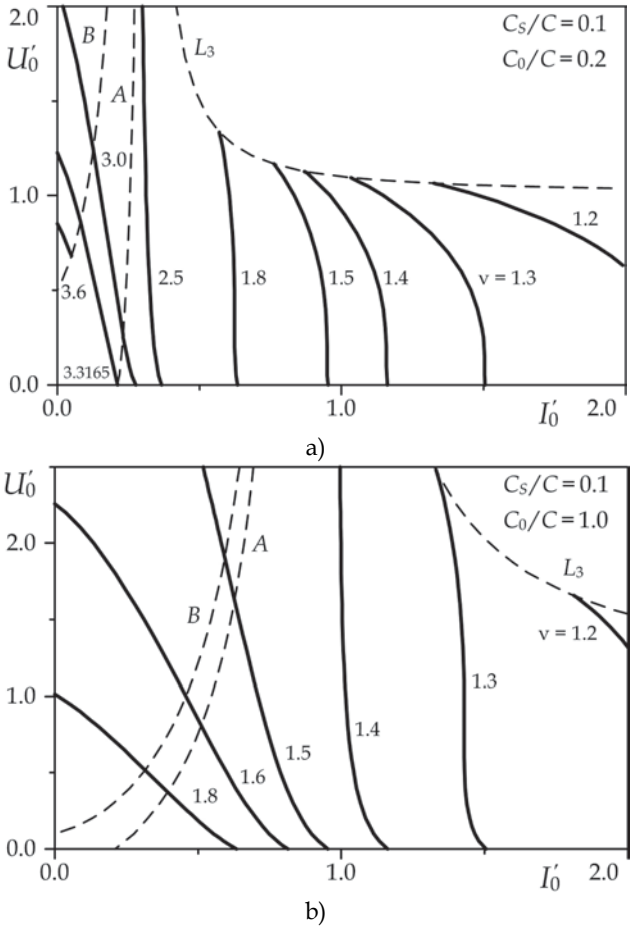

Fig. 7. Output characteristics of the LCC transistor DC/DC converter

Equations (12), (14) and (47) are substituted in condition (48), while equations (16) and (47) are substituted in condition (49). Then the inequalities (48) and (49) obtain the form:

$$I_0' \geq \frac{2\nu}{\pi} \cdot \frac{a_1 + a_2 U_0'}{1 + U_0'} \tag{50}$$

$$I_0' \geq \frac{2\nu}{\pi} \cdot \frac{a_1 - a_2 U_0'}{1 - U_0'} \tag{51}$$

Inequalities (50) и (51) enable with the possibility to draw the boundary curve *A* between the main and the medial modes of operation of the converter, as well as the border of the natural commutation – curve L_3 (fig. 7-a) or curve L_4 (fig. 7-b) in the plane of the output characteristics. It can be seen that the area of the main operation mode of the converter is limited within the boundary curves *A* and L_3 or L_4. The bigger the capacity of the capacitors

C_S and C_0, the smaller this area is. However, the increase of the snubber capacitors leads to a decrease in the commutation losses in the transistors as well as to limiting the electromagnetic interferences in the converter.

The expression (51) defines the borders, beyond which the converter stops working because of the breakage in the conditions for natural switching the controllable switches on at zero voltage (ZVS). Exemplary boundary curves have been drawn in the plane of the output characteristics (fig.8) at a_1=0.10. Four values have been chosen for the other parameter: a_2 = 0.05; 0.1; 0.2 and 1.0. When the capacity of the capacitor C_0 is smaller or equal to that of the snubber capacitors C_S $(a_1 \geq a_2)$, then the converter is fit for work in the area between the curve L_1 or L_2 and the x-axis (the abscissa). Only the main operation mode of the converter is possible in this area. The increase in the load resistance or in the operating frequency leads to stopping the operation of the converter before it has accomplished a transition towards the medial and the boundary modes of work.

When C_0 has a higher value than the value of C_S $(a_1 < a_2)$ then the boundary curve of the area of converter operation with ZVS is displaced upward (curve L_3 or L_4). It is possible now to achieve even a no-load mode.

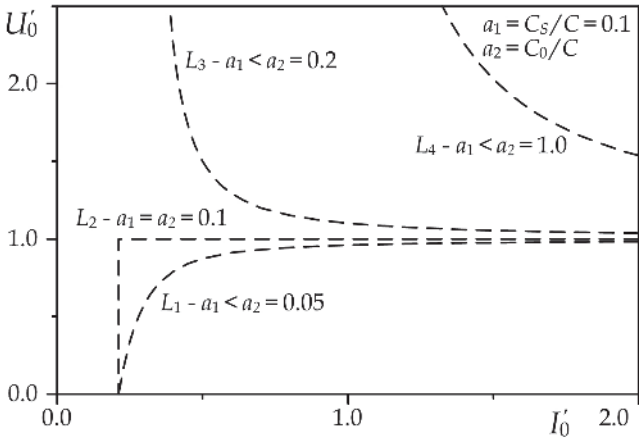

Fig. 8. Borders of the converter operation capability

4.2 Output characteristics and boundary curves at the boundary operation mode

Applying expression (47) for equations (35)÷(42) U'_{Cm} is eliminated. After that, by a consecutive substitution of expressions (35)÷(42) in equations (43)÷(45) as well as of expressions (43)÷(46) in equation (22), a dependence of the kind $U'_0 = f(I'_0, \nu, a_1, a_2)$ is obtained. Its solving enables with a possibility to build the outer (output) characteristics of the converter in relative units at the boundary operation mode under consideration and at regulation by changing the operating frequency. Such characteristics are shown in fig. 7-a for ν = 3.0; 3.3165; 3.6 and a_1=0.1; a_2=0.2 and in fig. 7-b for ν =1.5; 1.6; 1.8 and a_1=0.1; a_2=1.0.

At the boundary operation mode, the diodes of the rectifier have to start conducting after opening the freewheeling diodes of the inverter. This is guaranteed if the following condition is fulfilled:

$$x_4^0 \geq x_3^0 \tag{52}$$

After substitution of equations (39), (41) и (47) in the inequality (52), the mentioned above condition obtains the form:

$$I_0' \leq \frac{2\nu}{\pi} \cdot \frac{a_2 U_0' - a_1}{1 + U_0'} \tag{53}$$

Condition (53) gives the possibility to define the area of the boundary operation mode of the converter in the plane of the output characteristics (fig. 7-a and fig. 7-b). It is limited between the y-axis (the ordinate) and the boundary curve *B*. It can be seen that the converter stays absolutely fit for work at high-Ohm loads, including at a no-load mode. It is due mainly to the capacitor C_0. With the increase in its capacity (increase of a_2) the area of the boundary operation mode can also be increased.

5. Medial operation mode of the converter

At this operation mode, the diodes of the rectifier start conducting during the commutation in the inverter. The equivalent circuits, corresponding to this mode for a cycle, are shown in fig.9. In this case, the sinusoidal quantities have four different angular frequencies:

$\omega_0 = 1/\sqrt{LC}$ for stages 4 and 8;

$\omega_0' = 1/\sqrt{LC_{E1}}$, where $C_{E1} = CC_S/(C + C_S)$, for stages 3 and 7;

$\omega_0'' = 1/\sqrt{LC_{E2}}$, where $C_{E2} = CC_0/(C + C_0)$, for stages 1 and 5;

$\omega_0''' = 1/\sqrt{LC_{E3}}$, where $C_{E3} = CC_SC_0/(CC_S + CC_0 + C_SC_0)$, for stages 2 and 6.

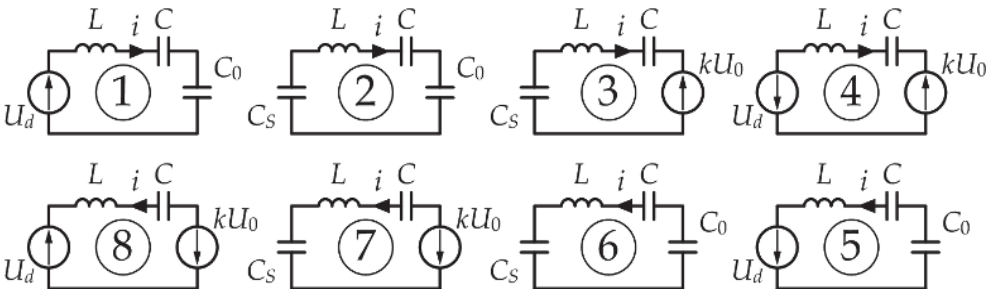

Fig. 9. Equivalent circuits at the medial operation mode of the converter

Therefore, the analysis of the medial operation mode is considerably more complex. The area in the plane of the output characteristics, within which this mode appears, however, is completely defined by the boundary curves *A* and *B* for the main and the boundary modes respectively. Having in mind the monotonous character of the output characteristics for the other two modes, their building for the mode under consideration is possible through linear interpolation. It is shown in fig. 7-a for ν = 3.0; 3.3165 as well as in fig. 7-b for ν=1.5; 1.6; 1.8. The larger area of this mode corresponds to the higher capacity of the snubber capacitors C_S and the smaller capacity of the capacitor C_0.

6. Methododlogy for designing the converter

During the process of designing the *LCC* resonant *DC/DC* converter under consideration, the following parameters are usually predetermined: power in the load $P_{0,}$ output voltage U_0 and operating frequency f. Very often, the value of the power supply voltage U_d is predefined and the desired output voltage is obtained by adding a matching transformer.
The design of the converter could be carried out in the following order:

1. Choice of the frequency distraction ν

For converters, operating at frequencies higher than the resonant one, the frequency distraction is usually chosen in the interval ν =1.1÷1.3. It should be noted here that if a higher value of ν is chosen, the exchange of reactive energy between the resonant circuit and the energy source increases, i.e., the current load on the elements in the circuit increases while the stability of the output characteristics decreases. It is due to the increase in the impedance of the resonant circuit of the converter.

2. Choice of the parameter $a_2 = C_0/C$

The choice of this parameter is a compromise to a great extent. On the one hand, to avoid the considerable change of the operating frequency during the operation of the converter from nominal load to no-load mode, the capacitor C_0 (respectively the parameter a_2) should be big enough. On the other hand, with the increase of C_0 the current in the resonant circuit increases and the efficiency of the converter decreases. It should be noted that a significant increase in the current load on the elements in the scheme occurs at $a_2 > 1$ (Malesani et al., 1995).

3. Choice of the parameter $a_1 = C_S/C$

The parameter a_1 is usually chosen in the interval a_1 = 0.02÷0.20. The higher the value of a_1 (the bigger the capacity of the damping capacitors), the smaller the area of natural commutation of the transistors in the plane of the output characteristics is. However, the increase in the capacity of the snubber capacitors leads to a decrease in the commutation losses and limitation of the electromagnetic interferences in the converter.

4. Choice of the coordinates of a nominal operating point

The values of the parameters a_1 and a_2 fully define the form of the output characteristics of the converter. The nominal operating point with coordinates I_0' and U_0' lies on the characteristic, corresponding to the chosen frequency distraction ν. It is desirable that this point is close to the boundary of natural commutation so that the inverter could operate at a high power factor (minimal exchange of reactive energy). If the converter operates with sharp changes in the load and control frequency, however, it is then preferable to choose the operating point in an area, relatively distant from the border of natural commutation. Thus, automatic switching the converter off is avoided – a function, integrated in the control drivers of power transistors.

5. Defining the transformation ratio of the matching transformer

The transformation ratio is defined, so that the required output voltage of the converter at minimal power supply voltage and at maximum load is guaranteed:

$$k \geq \frac{U_0' \cdot U_{d\min}}{U_0}, \tag{54}$$

where $U_{d\min}$ is the minimal permissible value of the input voltage U_d.

6. Calculating the parameters of the resonant circuit

The values of the elements in the resonant circuit L and C are defined by the expressions related to the frequency distraction and the output current in relative units:

$$\nu = \omega/\omega_0 = 2\pi f\sqrt{LC} \quad ; \quad I_0' = \frac{I_0/k}{U_d/\sqrt{L/C}} = \frac{P_0/k}{U_d U_0/\sqrt{L/C}} \tag{55}$$

Solving the upper system of equations, it is obtained:

$$L = \frac{k\nu U_d U_0 I_0'}{2\pi f P_0} \quad ; \quad C = \frac{\nu P_0}{2\pi f k U_d U_0 I_0'} \tag{56}$$

7. Experimental investigations

For the purposes of the investigation, a laboratory prototype of the LCC resonant converter under consideration was designed and made without a matching transformer and with the following parameters: power supply voltage $U_d = 500$ V; output power $P_0 = 2.6$ kW, output voltage $U_0 = 500$ V; operating frequency and frequency distraction at nominal load $f = 50$ kHz and $\nu = 1.3$; $a_1 = 0.035$; $a_2 = 1$; coordinates of the nominal operating point - $I_0' = 1.43$ and $U_0' = 1$. The following values of the elements in the resonant circuit were obtained with the above parameters: $L = 570$ μH; $C = C_0 = 30$ nF. The controllable switches of the inverter were IGBT transistors with built-in backward diodes of the type IRG4PH40UD, while the diodes of the rectifier were of the type BYT12PI. Snubber capacitors $C_1 \div C_4$ with capacity of 1 nF were connected in parallel to the transistors. Each transistor possessed an individual driver control circuit. This driver supplied control voltage to the gate of the corresponding transistor, if there was a control signal at the input of the individual driver circuit and if the collector-emitter voltage of the transistor was practically zero (ZVC commutation).

Experimental investigation was carried out during converter operation at frequencies $f = 50$ kHz ($\nu = 1.3$) and $f = 61.54$ kHz ($\nu = 1.6$). The dotted curve in fig.10 shows the theoretical output characteristics, while the continuous curve shows the output characteristics, obtained in result of the experiments.

A good match between the theoretical results and the ones from the experimental investigation can be noted. The small differences between them are mostly due to the losses in the semiconductor switches in their open state and the active losses in the elements of the resonant circuit.

Oscillograms, illustrating respectively the main and the boundary operation modes of the converter are shown in fig. 11 and fig. 12. These modes are obtained at a stable operating frequency $f = 61.54$ kHz ($\nu = 1.6$) and at certain change of the load resistor. In the oscillograms the following quantities in various combinations are shown: output voltage (u_a) and output current (i) of the inverter, input voltage (u_b) and output current (i_0) of the rectifier.

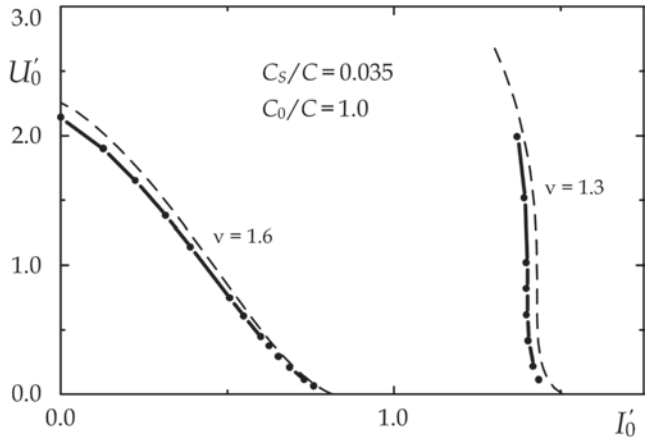

Fig. 10. Experimental output characteristics of the converter.

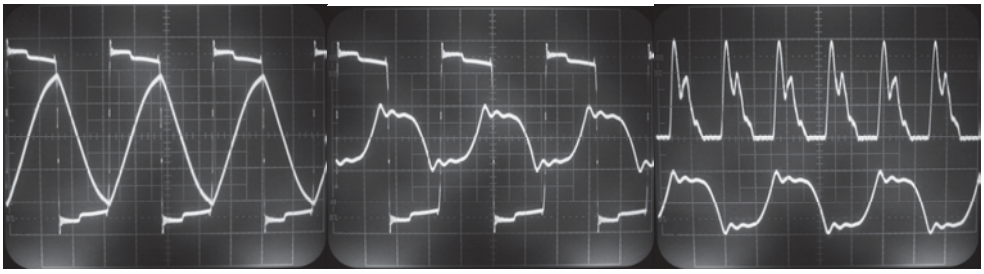

a) u_a 200 V/div; i 5 A/div; x=5μs/div

b) u_a 200V/div; u_b 200V/div; x=5μs/div

c) i_0 5A/div; u_b 200V/div; x=5μs/div

Fig. 11. Oscillograms illustrating the main operation mode of the converter

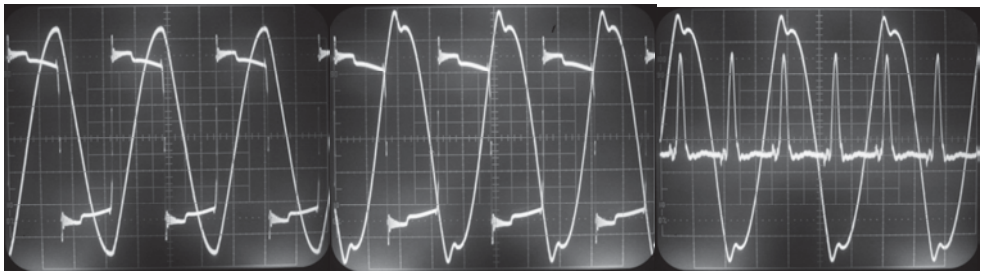

a) u_a 200V/div; i 5A/div; x=5μs/div

b) u_a 200V/div; u_b 200V/div; x=5μs/div

c) i_0 (5 A/div); u_b (200 V/div) x=5μs/div

Fig. 12. Oscillograms illustrating the boundary operation mode of the converter

From fig. 11-b and fig. 12-b the difference between the main and the boundary operation mode of the converter can be seen. In the first case, the commutations in the rectifier (the process of recharging the capacitor C_0) end before the commutations in the inverter (the process of recharging the capacitor C_S). In the second case, the commutations in the rectifier complete after the ones in the inverter. In both cases during the commutations in the rectifier, all of its diodes are closed and the output current i_0 is equal to zero (fig. 11-c and fig. 12-c).
Fig. 12-b confirms the fact that at certain conditions the output voltage can become higher than the power supply voltage without using a matching transformer.
At no-load mode, the converter operation is shown in fig. 13. In this case, the output voltage is more than two times higher than the power supply one.

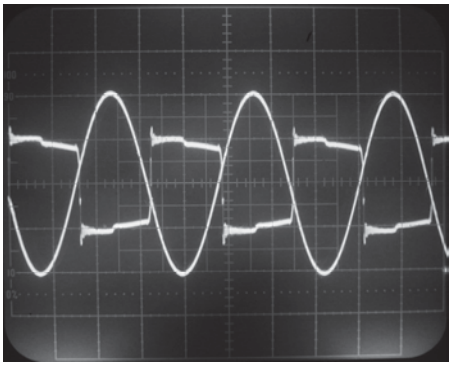

u_a 500V/div; u_b 500V/div; x=5μs/div

Fig. 13. Oscillograms, illustrating no-load mode of the converter

8. Conclusions

The operation of an LCC transistor resonant DC/DC converter with a capacitive output filter and working above the resonant frequency has been investigated, taking into account the influence of snubber capacitors and a matching transformer. The particular operation modes of the converter have been considered, and the conditions under which they are obtained have been described. The output characteristics for all operation modes of the converter have been built including at regulation by means of changing the operating frequency. The boundary curves between the different operation modes of the converter as well as the area of natural commutation of the controllable switches have been shown in the plane of the output characteristics. Results from investigations carried out by means of a laboratory prototype of the converter have been obtained and these results confirm the ones from the analysis.
The theoretical investigations show that the conditions for ZVS can be kept the same for high-Ohm loads and the converter can stay fit for work even at a no-load mode. For the purpose, it is necessary to have the natural capacity of the matching transformer bigger than the one of the snubber capacitors.
The output characteristics show that in the zone of small loads the value of the normalized output voltage increases to reach a value higher than unit what is characteristic for

converters with controllable rectifying. This can be explained by the similar mechanism of the rectifier operation in the investigated converter.
The results from the investigation can be used for more precise designing of LCC converters used as power supplies for electric arc welding aggregates, powerful lasers, luminescent lamps etc.

9. References

Al Haddad, K., Cheron, Y., Foch, H. & Rajagopalan, V. (1986). Static and dynamic analysis of a series resonant converter operating above its resonant frequency, *Proceedings of SATECH'86*, pp.55-68, Boston, USA.

Bankov, N. (2009) Influence of the Snubbers and Matching Transformer over the Work of a Transistor Resonant DC/DC Converter. *Elektrotehnika&Elektronika (Sofia, Bulgaria)*, Vol. 44, No. 7-8, pp. 62-68, ISSN 0861-4717.

Cheron, Y., Foch, H. & Salesses, J. (1985). Study of resonant converter using power transistors in a 25-kW X-Rays tube power supply. *IEEE Power Electronics Specialists Conference*, ESA Proceedings, 1985, pp. 295-306.

Cheron, Y. (1989). *La commutation douce dans la conversion statique de l'energie electrique*, Technique et Documentation, ISBN : 2-85206-530-4, Lavoisier, France.

Malesani, L., Mattavelli, P., Rossetto, L., Tenti, P., Marin, W. & Pollmann, A. (1995). Electronic Welder With High-Frequency Resonant Inverter. *IEEE Transactions on Industry Applications*, Vol. 31, No.2, (March/April 1995), pp. 273-279, ISSN: 0093-9994.

Jyothi, G. & Jaison, M. (2009). Electronic Welding Power Source with Hybrid Resonant Inverter, *Proceedings of 10th National Conference on Technological Trends (NCTT09)*, pp. 80-84, Kerala, India, 6-7 Nov 2009.

Liu, J., Sheng, L., Shi, J., Zhang, Z. & He, X. (2009). Design of High Voltage, High Power and High Frequency in LCC Resonant Converter. *Applied Power Electronics Conference and Exposition, APEC 2009. Twenty-Fourth Annual IEEE*, pp. 1034-1038, ISSN: 1048-2334, Washington, USA, 15-19 Feb. 2009.

Ivensky, G., Kats, A. & Ben-Yaakov, S. (1999). An RC load model of parallel and series-parallel resonant DC-DC converters with capacitive output filter. *IEEE Transactions on Power Electronics*, Vol. 14, No.3, (May 1999), pp. 515-521, ISSN: 0885-8993.

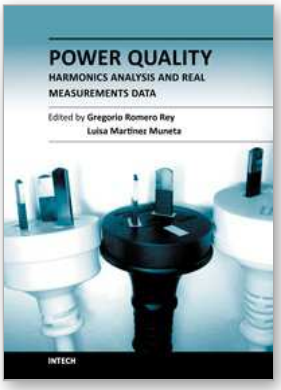

Power Quality Harmonics Analysis and Real Measurements Data
Edited by Prof. Gregorio Romero

ISBN 978-953-307-335-4
Hard cover, 278 pages
Publisher InTech
Published online 23, November, 2011
Published in print edition November, 2011

Nowadays, the increasing use of power electronics equipment origins important distortions. The perfect AC power systems are a pure sinusoidal wave, both voltage and current, but the ever-increasing existence of non-linear loads modify the characteristics of voltage and current from the ideal sinusoidal wave. This deviation from the ideal wave is reflected by the harmonics and, although its effects vary depending on the type of load, it affects the efficiency of an electrical system and can cause considerable damage to the systems and infrastructures. Ensuring optimal power quality after a good design and devices means productivity, efficiency, competitiveness and profitability. Nevertheless, nobody can assure the optimal power quality when there is a good design if the correct testing and working process from the obtained data is not properly assured at every instant; this entails processing the real data correctly. In this book the reader will be introduced to the harmonics analysis from the real measurement data and to the study of different industrial environments and electronic devices.

How to reference
In order to correctly reference this scholarly work, feel free to copy and paste the following:

Nikolay Bankov, Aleksandar Vuchev and Georgi Terziyski (2011). Study of LCC Resonant Transistor DC / DC Converter with Capacitive Output Filter, Power Quality Harmonics Analysis and Real Measurements Data, Prof. Gregorio Romero (Ed.), ISBN: 978-953-307-335-4, InTech, Available from: http://www.intechopen.com/books/power-quality-harmonics-analysis-and-real-measurements-data/study-of-lcc-resonant-transistor-dc-dc-converter-with-capacitive-output-filter

INTECH
open science | open minds

InTech Europe
University Campus STeP Ri
Slavka Krautzeka 83/A
51000 Rijeka, Croatia
Phone: +385 (51) 770 447
Fax: +385 (51) 686 166
www.intechopen.com

InTech China
Unit 405, Office Block, Hotel Equatorial Shanghai
No.65, Yan An Road (West), Shanghai, 200040, China
中国上海市延安西路65号上海国际贵都大饭店办公楼405单元
Phone: +86-21-62489820
Fax: +86-21-62489821